Dagmar Chudobova[1,2]
Kristyna Cihalova[1,2]
Sylvie Skalickova[1,2]
Jan Zitka[1,2]
Miguel Angel Merlos Rodrigo[1,2]
Vedran Milosavljevic[1,2]
David Hynek[1,2]
Pavel Kopel[1,2]
Radek Vesely[3]
Vojtech Adam[1,2]
Rene Kizek[1,2]

[1]Department of Chemistry and Biochemistry, Mendel University in Brno, Brno, Czech Republic
[2]Central European Institute of Technology, Brno University of Technology, Technicka, Brno, Czech Republic
[3]Department of Traumatology, Faculty of Medicine, Masaryk University, Trauma Hospital of Brno, Ponavka, Brno, Czech Republic

Received July 4, 2014
Revised July 22, 2014
Accepted July 22, 2014

Research Article

3D-printed chip for detection of methicillin-resistant *Staphylococcus aureus* labeled with gold nanoparticles

Methicillin-resistant *Staphylococcus aureus* (MRSA) is a dangerous pathogen occurring not only in hospitals but also in foodstuff. Currently, discussions on the issue of the increasing resistance, and timely and rapid diagnostic of resistance strains have become more frequent and sought. Therefore, the aim of this study was to design an effective platform for DNA isolation from different species of microorganisms as well as the amplification of *mecA* gene that encodes the resistance to β-lactam antibiotic formation and is contained in MRSA. For this purpose, we fabricated 3D-printed chip that was suitable for bacterial cultivation, DNA isolation, PCR, and detection of amplified gene using gold nanoparticle (AuNP) probes as an indicator of MRSA. Confirmation of the MRSA presence in the samples was based on a specific interaction between *mecA* gene with the AuNP probes and a colorimetric detection, which utilized the noncross-linking aggregation phenomenon of DNA-functionalized AuNPs. To test the whole system, we analyzed several real refractive indexes, in which two of them were positively scanned to find the presence of *mecA* gene. The aggregation of AuNP probes were reflected by 75% decrease of absorbance ($\lambda = 530$ nm) and change in AuNPs size from 3 ± 0.05 to 4 ± 0.05 nm ($n = 5$). We provide the one-step identification of *mecA* gene using the unique platform that employs the rapid, low-cost, and easy-to-use colorimetric method for MRSA detection in various samples.

Keywords:
3D-printed chip / Gold nanoparticles / Methicillin resistant / Pathogen detection / *Staphylococcus aureus*
DOI 10.1002/elps.201400321

1 Introduction

Staphylococcus aureus is a Gram-positive abundantly occurring bacterium, while methicillin-resistant *S. aureus* (MRSA) is a live-threatening pathogen occurring mainly in hospitals [1, 2]. In the period between 2011 and 2012, MRSA was reported in 41.2% of *S. aureus* isolated and typed in healthcare-associated infections in European hospitals [3]. From this it is clear that MRSA was and still is primarily considered as a healthcare-associated pathogen, however, later on, these bacteria were also detected in food products, especially in meats [4]. Therefore, these bacteria can be isolated both from inpatients as well as people not related to medical environment, and this epidemiological change is important in distribution of infections caused by this pathogen [5].

The design and fabrication of new diagnostic systems necessitates working in collaboration between different disciplines. Recent PCR-based assays for MRSA identification have significantly reduced the time needed to find a diagnosis for a patient [6, 7]. Most importantly, small, field-capable analysis portable systems are critical for timely detection and prevention efforts even in the case of MRSA. Thus, rapid and inexpensive diagnostic systems with high sensitivity and specificity are essential to prevent MRSA to be an emerging public health threat. There are different techniques such as optical, mechanical, magnetic, and electrochemical, and their combinations in detection of biologically related analytes. In labeling strategies, fluorescent dye molecules, quantum dot labels, and metal colloid labels are generally used [8–10]. Recent results show that combining the advantages of microelectromechanical system technology and molecular methods is promising for detection of MRSA [11]. The integration of magnetic bead based detection with loop-mediated

Correspondence: Dr. Rene Kizek, Department of Chemistry and Biochemistry, Mendel University in Brno, Zemedelska 1, CZ-613 00 Brno, Czech Republic
E-mail: kizek@sci.miuni.cz
Fax: +420-5-4521-2044

Abbreviations: **AuMNP**, gold magnetic nanoparticle; **AuNP**, gold nanoparticle; **CV**, cyclic voltammetry; **MRSA**, methicillin-resistant *Staphylococcus aureus*; **SECM**, scanning electrochemical microscopy

Colour Online: See the article online to view Figs. 1–4 in colour.

isothermal amplification process was recently studied by Wang et al. The hybridization was conducted using magnetic bead conjugated complementary probes. Cell lysis, DNA isolation, and amplification using loop-mediated isothermal amplification technique were performed in the microfluidic device only [12]. From these mentioned facts, it follows that there is a great development in the field of manufacturing well portable devices for medical purposes.

Thus, the main objective of this study was to suggest and construct a novel integrated microfluidic platform for rapid and accurate detection of MRSA strain. This platform is capable of colorimetric determination of the target analyte in a microfluidic reactor, rendering its usefulness for in vitro diagnostics. Confirmation of the MRSA presence in the samples is based on isolation of DNA, amplification of *mecA* gene encoding the resistance to β-lactam antibiotics, and specific interaction between *mecA* gene with the gold nanoparticle (AuNP) probes and a colorimetric detection, which utilized the noncross-linking aggregation phenomenon of DNA-functionalized AuNPs.

2 Materials and methods

2.1 Chemicals, preparation of DI water, and pH measurement

Chemicals used in this study were purchased from Sigma-Aldrich (St. Louis, USA) in ACS purity unless noted otherwise. The DI water was prepared using reverse osmosis equipment Aqual 25 (Czech Republic). The DI water was further purified using apparatus MiliQ Direct QUV equipped with the UV lamp. The resistance was 18 MΩ. The pH was measured using pH meter WTW inoLab (Weilheim, Germany).

2.2 Cultivation of bacteria strains

Nonresistant strains (*S. aureus, Escherichia coli, Salmonella typhimurium, and Lactobacillus rhamnosus* and resistant strains of *S. aureus* (MRSA) were obtained from the Czech Collection of Microorganisms, Faculty of Science, Masaryk University, Brno, Czech Republic. The strains were stored as a spore suspension in 20% v/v glycerol at −20°C. Prior to use in this study, the strains were thawed and the glycerol was removed by washing with distilled water. The composition of cultivation medium was as follows: tryptone 10 g/L, yeast extract 5 g/L, NaCl 5 g/L, pH of the cultivation medium was adjusted at 7.4 before sterilization. The sterilization of the media was carried out at 121°C for 30 min in sterilizer (Tuttnauer 2450EL, Beit Shemesh, Israel). The prepared cultivation media were inoculated with bacterial culture into 25 mL Erlenmeyer flasks. After inoculation, the bacterial cultures were cultivated for 24 h in a shaker at 600 rpm and 37°C.

2.3 Preparation of hospital samples and their cultivation

2.3.1 Wound swabs of patients with bacterial infections

Clinical specimens including wound swabs were obtained from Trauma Hospital of Brno, Czech Republic. There were selected patients aged less than 60 years without diagnosis of diabetes mellitus, peripheral arterial disease, nonsmoker, not under corticosteroid treatment or immunosuppressant in regular medication. The smears were taken from infected wounds with the consent of patients. Particularly, smear was made from a patient with perianal abscess before the medical treatment, during treatment using Biseptol (Pabianickie Zaklady Farmaceutyzcne Polfa S.A., Pabianice, Poland), and at regular intervals after completion of the treatment. Smear was done by rolling motion at the site of skin puncture using a sterile swab sampling. The swab was then placed into a tube with a semisolid transport medium and carefully sealed and labeled. Marked tubes were immediately microbiologically examined. The swab sample was left in the transport medium intended for the storage of the sample before culturing in the appropriate medium.

2.3.2 Cultivation of clinical specimens

The isolation of bacterial strains from hospital samples was performed using selective blood agar. The swab sample was cultivated on blood agar with 10% of NaCl, blood agar without other compounds [13], Endo agar [14], and blood agar with amikacin [15]. These Petri dishes were cultivated for 24–48 h in 37°C. The identification of bacterial strains isolated from hospital samples was done using MALDI-TOF MS [16]. The MS experiments were performed on a MALDI-TOF/TOF mass spectrometer Bruker Ultraflextreme (Bruker, Bremen, Germany) equipped with a laser (Bruker) operating at wavelength of 355 nm with an accelerating voltage of 25 kV, cooled with nitrogen, and a maximum energy of 43.2 μJ with repetition rate 2000 Hz in linear and positive mode, and with software for data acquisition and processing of mass spectra flexControl version 3.4 and flexAnalysis version 2.2. A sample of 500 μL *S. aureus* (0.1 OD) culture cultivated overnight was centrifuged at 14 000 × *g* for 2 min. After that, supernatant was discarded and the pellet was suspended in 300 μL of DI water. Then, 900 μL of ethanol was added. After centrifugation at 14 000 × *g* for 2 min, supernatant was discarded and obtained pellet was air-dried. The pellet was then dissolved in 25 μL of 70% formic acid v/v and 25 μL of ACN, and was mixed. The samples were centrifuged at 14 000 × *g* for 2 min and 1 μL of the clear supernatant was spotted in duplicate onto the MALDI target (MTP 384 target polished steel plate; Bruker Daltonics, Bremen, Germany) and air-dried at a room temperature. Then, each spot was overlaid with 1 μL of α-cyano-4-hydroxycinnamic acid matrix solution saturated with organic solvent (50% ACN and 2.5%

TFA, both v/v) and air-dried completely prior to MALDI-TOF MS measurement. Spectra were taken in the *m/z* range of 2000–20 000 Da, and each was a result of the accumulation of at least 1000 laser shots obtained from ten different regions of the same sample spot. Prior to analysis, the mass spectrometer was externally calibrated with a peptide mix of bombesin, angiotensin I, glu-fibrinopeptide B, adrenocorticotropic hormone, ubiquitine, and cytochrome c. Spectra with peaks outside the allowed average were not considered. Modified spectra were loaded into the MALDI BioTyper™ 3.1 Version (Bruker Daltonik, Bremen, Germany).

2.4 Synthesis of AuNPs and gold magnetic nanoparticles (AuMNPs)

Water-soluble AuNPs were synthesized as follows. Ten milliliters of 1 mM $HAuCl_4 \cdot 3H_2O$ was added to a 50 mL beaker under magnetic stirring. Aqueous solution of sodium citrate tribasic dihydrate (0.5 mL, 40 mM) was added to $HAuCl_4 \cdot 3H_2O$ solution. The color of the solution slowly changed from yellow to violet. Mixture was left for stirring overnight.

The AuMNPs were prepared according to the following procedure. Two different solutions were prepared separately: (i) 1.5 g of $Fe(NO_3)3 \cdot 9H_2O$ was dissolved in 80 mL of water in a 250 mL beaker and (ii) 1.4 mL of 25% NH_3 v/v solution was mixed with 8.6 mL of water in a screw-capped tube and poured in a separate beaker. A total of 0.2 g of $NaBH_4$ was mixed with the second solution. A magnetic rotor was used to mix them properly. After 10 min of mixing, the solution was added to the first solution. The color of the solution became black with an initial frothing. Then, it was heated at 100°C for 2 h. The mixture was stirred overnight. Next day, the magnetic particles were separated from the solution by an external magnet and washed several times with DI water. Maghemite nanoparticles were prepared from 1.5 g $Fe(NO_3)_3 \cdot 9H_2O$, as a source of iron was suspended in 80 mL of water and PVP (10 k, 1.5 g in 20 mL of water) was added with stirring. After 3 h of stirring, a solution of $HAuCl_4$ (25 mL, 1 mM) was added. The solution was stirred for 1 h and a solution of trisodium citrate dihydrate (0.75 mL, 0.265 g/10 mL) was added. The solution was stirred overnight, separated by magnet, washed with DI water, and dried at 40°C. Finally, the magnetic AuNPs were air-dried and stored in a glass container.

2.5 Characterization of AuMNPs and AuNPs by SEM

Structure of 3 mM AuMNPs and 1 mM AuNPs was characterized by SEM. For documentation of the nanoparticle structures, a MIRA3 LMU (Tescan, Brno, Czech Republic) was used. This model is equipped with a high brightness Schottky field emitter for low noise imaging at fast scanning rates. The SEM was fitted with in-beam SE detector. Samples were coated by 5 nm of platinum to prevent sample charging. For automated acquisition of selected areas, a TESCAN proprietary software tool called Image Snapper was used. The software enabled automatic acquisition of selected areas with defined resolution. An accelerating voltage of 15 kV and beam currents about 1 nA gave satisfactory results regarding maximum throughput. Magnification for AuMNPs 40 kX, AuNPs 40.9 kX, and aggregated AuNPs 64.6 kX were used.

2.6 Nanoparticles' surface characterization by scanning electrochemical microscope

Surface of AuMNPs and AuNPs was measured by scanning electrochemical microscope (SECM) Model 920C (CH Instruments, Austin, TX, USA). The electrochemical microscope consisted of a 10 μm platinum disc probe electrode, which was controlled by piezoelectric motors driven by all three axes. Electrochemical measurements were performed in a three-electrode configuration using platinum wire as a counterelectrode and Ag/AgCl/ 3 M KCl as a reference electrode. During scanning, the particles were attached on the substrate platinum electrode by magnetic force from neodymium magnet, situated below the electrode. The surfaces were characterized by cyclic voltammetry (CV) in 3 M KCl and 1 mM $FcCH_2OH$ using following parameters—initial potential: 0.2 V, high potential: 0.5 V, and low potential: −0.2 V. Initial scan polarity was positive with scan rate 0.02 V/s. Quiet time was 10 s. Electrochemical scanning method was carried out with potential of working microelectrode of 0.2 V. Gold disc electrodes with an O-ring as the conducting substrate used potential of 0.3 V. Speed of scanning was 250 μm/s. The platinum-measuring electrode moved at least 50 μm above the surface.

2.7 X-ray fluorescence analysis

Qualitative analysis of AuNPs and AuMNPs was measured on Spectro Xepos (Spectro Analytical Instruments, Kleve, Germany). The sample was measured on a Pd anode X-ray tube working at a voltage of 47.63 kV and a current of 0.5 mA, and detected with Barkla scatter aluminum oxide. Measurement time was 300 s. For excitation, an Mo secondary target was used. The excitation geometry was 90°. The AuNPs were measured through the PE bottle side wall 20 mm above the bottom. The Spectro Xepos software and TurboQuant method were applied for data treatment.

2.8 Characterization of nanoparticles' size

The average nanoparticles' size and size distribution were determined by quasielastic laser light scattering with a Malvern Zetasizer (NANO-ZS, Malvern Instruments, Worcestershire, UK). Nanoparticle distilled water solution of 1.5 mL (1 mg/mL) was put into a polystyrene latex cell and measured at detector angle of 173°, wavelength of 633 nm, refractive

index of 0.30, real refractive index of 1.59, and temperature of 25°C.

2.9 Labeling of nanoparticles

The AuNPs and AuMNPs were labeled with thiolated mecA primers 5′-[ThiC6]CCCAATTTGTCTGCCAGTTT-3′ in the case of AuNPS and 5′-[ThiC6]TGGCAATATTAACG CACCTC-3′ in the case of AuMNPs. The protocol was as follows. Ninety microliters of AuNPs was mixed with 10 μL of 100 μM thiolated mecA primers and incubated for 24 h in 4°C.

2.10 Reverse transcription and amplification of *mecA* gene

2.10.1 Thermolysis of bacteria and reverse transcription of mRNA

The lysis of the bacteria was done by heat treatment (99°C) during 30 min. The mRNA was converted to cDNA using PrimeScript One Step RT-PCR Kit (TaKaRa, Mountain View, CA, USA). The reaction profile was as follows: initial denaturation at 94°C for 2 min, 30 cycles of 94°C for 30 s, 50°C for 30 s, and 72°C for 1.5 min.

2.10.2 Binding of DNA with magnetic AuNPs

Ten microliters of paramagnetic particles were washed three times with phosphate buffer (0.1 M NaCl, 0.05 M Na_2HPO_4, and 0.05 M NaH_2PO_4). After that, 10 μL of cDNA and 10 μL of immobilization buffer were added (0.1 M Na_2HPO_4, 0.1 M NaH_2PO_4, 0.6 M guanidinium thiocyanate, 0.15 M Tris-HCl (pH 7.5), and 2.5 M CsCl). This solution was kept for next 1.5 h at 20°C with shaking to bind DNA with magnetic AuNPs. Further, the solution was removed and magnetic AuNPs were washed two times with 20 μL of 5 M NaCl. The obtained magnetic AuNPs with DNA were resuspended in DI water.

2.10.3 PCR and electrophoresis in agarose gel

Taq PCR kit and cDNA (New England Bio-Labs, USA) were used for amplification of MRSA *mecA* gene DNA fragment. The sequences of forward and reverse primers selected from the nucleotide database of NCBI website were 5′-CCC AATTTGTCTGCCAGTTT-3′ and 5′-TGGCAATATTAACGC ACCTC-3′ (Sigma-Aldrich), respectively. Briefly to the experimental protocol, 25 μL of reaction mixture was composed of 1× standard *Taq* reaction buffer, 0.2 mM dNTPs, 0.2 μM primers, 1.25 U *Taq* DNA polymerase, and 10 μL of DNA. PCR was carried out in a thermocycler Mastercycler ep realplex 4S (Eppendorf, Hamburg, Germany) with the following temperature program: initial denaturation at 95°C for 120 s, 25 cycles of denaturation at 95°C for 15 s, annealing at 55°C for 30 s, extension at 72°C for 45 s, and a final extension at 72°C for 5 min. The resulting DNA fragment (113 bp) was electrophoresed in 1.8% m/v agarose gel (Mercury, USA) in 1× TAE buffer (40 mM Trizma-base, 20 mM acetic acid, and 1 mM EDTA, pH 8.0). A DNA ladder (New England BioLabs, USA), within the range from 0.1 to 1.5 kbp, was used as a standard to monitor the size of the analyzed fragments of DNA. The electrophoresis (Bio-Rad, USA) was run at 70 V and 6°C for 135 min. After electrophoresis, the gel was stained with ethidium bromide (31.3 ng/L) in 1× TAE buffer. Bands were visualized using a transilluminator at a wavelength of 312 nm (Vilber-Lourmat, Marne-la-Valle´e, France). Visualized image was recorded by a digital camera Canon G10 (Canon, Japan).

2.11 Confirmation of *mecA* gene in nonresistant and resistant bacterial strains

2.11.1 Isolation of DNA

For analysis of *mecA* gene, 2 mL each of the tested strains (*S. aureus*, MRSA, *E. coli*, *S. typhimurium*, and *L. rhamnosus*) were centrifuged (5000 × *g*, 20°C, 10 min). Lysis was done for 1 h in 400 μL of lysis solution (6 M guanidine hydrochloride and 0.1 M sodium acetate) at 20°C. The isolation of genomic DNA was performed using MagNA Pure Compact (Roche, Germany).

2.11.2 Amplification of DNA for *mecA* gene

The 16S rRNA and *mecA* genes were amplified using multiplex PCR. The sequences of forward and reverse primers of 16S rRNA gene were 5′-GAGTTTGATCCTGGCTCAG-3′ and 5′-GGTTACCTTGTTACGACTT-3′; respectively, and *mecA* primers were 5′-CCCAATTTGTCTGCCAGTTT-3′ and 5′-TGGCAATATTAACGCACCTC-3′, respectively. The final volume of the PCR reaction mixture was 25 μL. The reaction profile was as follows: 94°C for 4 min, 30 cycles of 94°C for 30 s, 52°C for 30 s, and 68°C for 90 s, and a final extension at 68°C for 7 min. The amplification was carried out using Mastercycler ep realplex 4S (Eppendorf) and 1498 bp fragment for 16S rRNA gene and 223 bp fragment for *mecA* gene.

2.11.3 Visualization of the amplified genes

DNA was mixed with loading buffer and then pipetted into the wells, and run in 1.5% agarose gel electrophoresis in 1× TAE buffer with ethidium bromide for 90 min at 90 V. The bands were visualized by UV transilluminator at 312 nm (Vilber-Lourmat) and band intensities were quantified and analyzed by Carestream Molecular Imaging Software (Carestream, Carestream In vivo Xtreme Imaging System, Rochester, USA) and normalized to *mecA* gene control.

2.12 Detection of *mecA* gene fragment or bacterial DNA using AuNPs probe

Absorbance spectra were acquired by multifunctional microplate reader Tecan Infinite 200 PRO (TECAN, Switzerland). The absorbance scan was measured within the range from 230 to 1000 nm per 5 nm steps. Each absorbance value was an average of three measurements. The detector gain was set to 100. The sample (2 μL) was placed in 16-well nanoplate by Tecan NanoQuant plate (TECAN). All measurements were performed at 25°C controlled by Tecan Infinite 200 PRO (TECAN). Ten microliters of AuNPs probe and 10 μL of AuMNPs probe were mixed with 5 μL of PCR product (26 μM). Afterwards the mixture was heated for 5 min at 95°C and slowly cooled to 25°C. For the *mecA* gene detection, 10 μL of 5 M NaCl was added into the cooled mixture (to final concentration of 2 M).

2.13 3D-printed chip design and fabrication

For bacterial cultivation, lysis, DNA isolation, PCR, and detection the 3D-printed chip was fabricated using 3D printer (Profi3Dmaker, Aroja, Czech Republic) controlled by G3Dmaker v1.0 software (Aroja). The reaction chamber was made from acrylonitrile butadiene styrene (Printplus, Aroja), which is sufficiently rigid and wiry for the final application of the product. The material had also the following properties such as small water absorption and resistance to oils, acids, alkalis, and hydrocarbons. The sample was injected into the chip using programmed syringe pump (Model eVol, SGE Analytical Science, Australia), three-way two-position selector valve (made from six-way valve, Valco, Instruments, USA), and dosing capillary, which was moved into the reaction chamber. To prepare a fully automated system, switching valve enabling switching between the off-waste and sample flow was placed into the system. The sample (10–500 μL) was injected by automated syringe (SGE Analytical Science, Australia) using maximal applied speed of 1.66 μL/s. Mobility and stirring of sample inside chip was arranged using multiturn magnet regulated on working current 200 mA, voltage 12 V, and 1 Hz pulse/frequency. The entire chip is enclosed in a thermostatic box equipped with fan, heater element, and temperature sensor. The heating element was driven by temperature sensors feedback (Instrumentation Temperature Controller, Valco, Instruments). The temperature was automatically operated by control unit Arduino Due (Atmel, USA). Flow measurement chamber in volume of 750 μL fitted with a spectrophotometric detector was used for the final sample absorbance measurement. The detector consists of LED bulb (Roithner Laser, Austria), band-pass filter (Semrock, USA) for 530 nm, and photodiode (Hamamatsu, Japan). All measurements were controlled by Arduino board Due (Atmel) and Arduino IDE (Atmel).

2.14 Descriptive statistics

Mathematical analysis of the data and their graphical interpretation were realized by Microsoft Excel®, Microsoft Word®, Microsoft PowerPoint® (USA), and STATISTICA.CZ (Czech Republic). Results are expressed as mean ± SD unless noted otherwise (EXCEL®).

3 Results and discussion

3.1 Characterization of AuMNPs and nonaggregated or aggregated AuNPs

The used nanoparticles play the crucial role for analysis inside the chip. Using the AuMNPs, the mobility and stirring of solution are ensured. Afterwards the AuNPs provide the spectrophotometric detection of *mecA* gene employing their aggregation in the presence of NaCl [17]. For our experiments, we characterized our fabricated AuMNPs, AuNPs, as well as AuNPs in NaCl presence from the point of view of surface analysis [18], electrochemical properties of particles [19, 20], qualitative analysis [21, 22], and measurement of size and zeta potential [23, 24].

At first, we characterized the AuMNPs by SEM. Iron oxide nanoparticles formed clusters of irregular shape in neutral pH (Fig. 1A, i). In order to image the reduction and oxidation properties of AuMNPs, CV of AuMNPs and surface scans were measured by SECM and the resulting maps are shown in Fig. 1A, ii. The CV scan of AuMNPs provided the lowest reduction signal in comparison to other studied particles. The oxidation potential was determined as 0.3 V, whereas the reduction potential as 0.15 V. From SECM map, it is obvious that the surface current is within the range from 0.6 to 0.9 nA. The qualitative analysis and impurities determination confirm the purity of AuMNPs, which contained bulk of Au^{+} and Fe^{3+} ions (data not shown). Finally, we characterized size and zeta potential of magnetic particles. It is shown in Fig. 1A, iii that the size of these particles was found to be 15 ± 3 nm. To confirm that these magnetic nanoparticles carry negative charges, measurement of the zeta potential (or charge density) of samples was done providing important information for predicting their binding capacity. The zeta potential of magnetic nanoparticles covered with gold (19 mV) was found to be higher than that of AuNPs (−25 mV). This indicates that part of citrate on gold surface, which was used for reduction and protection of AuNPs from aggregation, was bounded with iron oxide by covalent bond resulting in increasing of zeta potential and decreasing of free citrate on gold surface.

The SEM characterization of AuNPs is demonstrated in Fig. 1B, i. It follows from the results obtained that AuNPs were spherical and cuboid in shape. CV scan of AuNPs surface shows the oxidation potential at 0.4 V and reduction potential at 0.25 V. In addition, SECM map revealed us AuNPs current within the range from −0.2 to −0.4 nA (Fig. 1B, ii). The qualitative analysis of AuNPs confirmed the presence of trace amount of chloride ions present due to its preparation

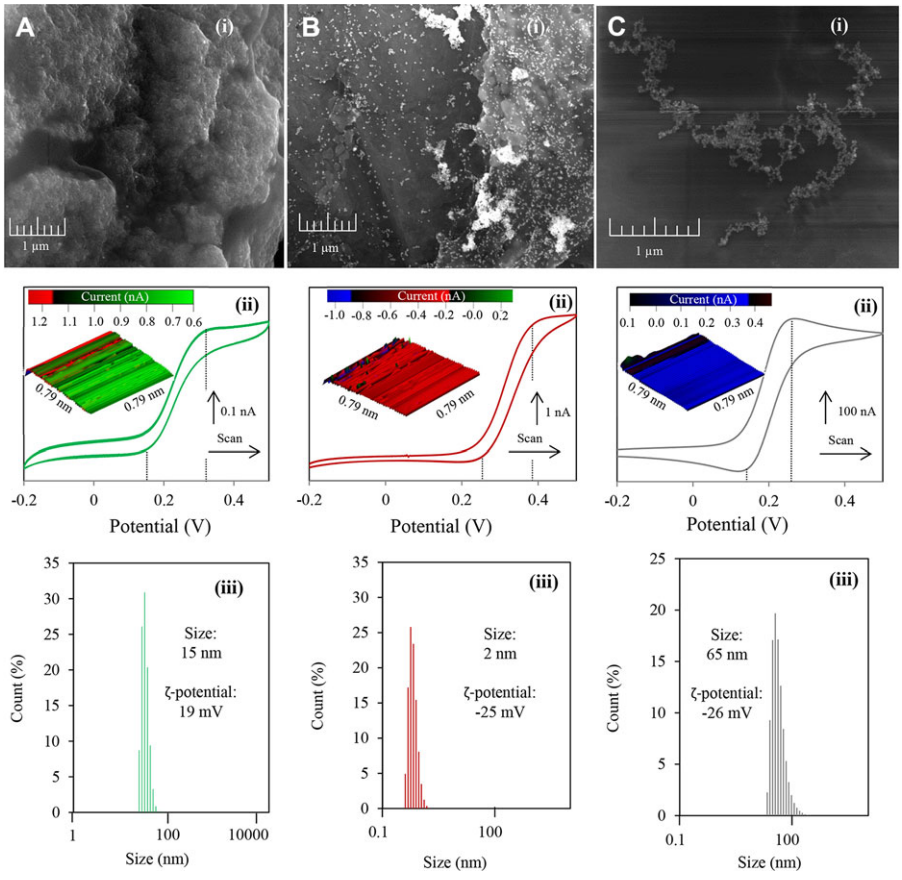

Figure 1. Microscopic and electrochemical characterization of (A) 1 mg/mL AuMNPs, (B) 1 mg/mL AuNPs, and (C) aggregated 1 mg/mL AuNPs dissolved in water by (i) SEM (magnification of 40 kX for AuMNPs, 40.9 kX for AuNPs, and 64.6 kX for aggregated AuNPs), (ii) scanning electrochemical microscope (0.3 V potential of measurement, 250 μm/s speed of scanning, and 50 μm height above the surface), and (iii) the measurements of AuNPs size distribution by Zetasizer. Measuring conditions were: detector angle 173°, wavelength 633 nm, refractive index 0.30, a real refractive index 1.59, and a temperature 25°C.

(data not shown). Moreover, the size of AuNPs was found to be 2 ± 0.5 nm and zeta potential −25 mV (Fig. 1B, iii).

Using the SEM it was found that the AuNPs in the presence of NaCl formed irregular clusters in comparison with AuNPs (Fig. 1C, i). The observation of oxidation or reduction properties of AuNPs in the presence of NaCl demonstrated the oxidation potential as 0.25 V and reduction potential as 1.4 V. Particularly, CV analysis showed higher reduction/oxidation properties in comparison with AuNPs, which could be caused by the increase of particle surface due to particles aggregation. SECM scanning map of AuNPs illustrated the change of surface current within the range from 0.1 to 0.3 nA probably associated with AuNPs aggregation, which is in agreement with CV results (Fig. 1C, ii). Characterization proved that the AuNPs agglomeration and size of these particles were found to be 65 ± 35 nm. Summarization of zeta potential values showed that AuNPs had the lowest zeta potential at −26 mV due to its permanent negative charges (Fig. 1C, iii). Based on all characterizing results obtained, it can be concluded that the particles have the ability to be used for DNA binding and colorimetric detection as other commercial nanoparticles.

3.2 Confirmation of resistance gene presence in different bacterial strains

Scheme in Fig. 2A shows the isolation and confirmation of *mecA* resistance gene expression present in MRSA. mRNA from bacterial culture proliferating for 24 h under constant conditions was transcribed using reverse transcription into cDNA and isolated using magnetic particles. The *mecA* gene encoding the resistance to the β-lactam antibiotics was amplified and amplicon in response to the absorbance of bacterial culture before isolation (expressed in absorbance values (λ = 600 nm) 0.0005, 0.005, 0.01, 0.05, 0.1, 0.5, 1 AU) is shown in gels (Fig. 2B). The decreasing intensity of bands (*mecA* fragment, 223 bp) in the gel with the decreasing concentration of MRSA was demonstrated (Fig. 2C).

To confirm the 16S rRNA gene expression, which is naturally present in all bacterial strains, and *mecA* resistance gene, there were selected different bacterial strains of nonresistant *S. aureus*, MRSA, *E. coli*, *S. typhimurium*, *L. rhamnosus* (sample numbers 1–5), and three bacterial strains isolated from the clinical specimens from patients with bacterial infections identified as *S. aureus* (sample numbers 6–8, Fig. 2D). 16S gene expression was expectedly confirmed in all the tested bacterial strains. In the studies [25, 26], the 16S rRNA gene for classification and identification of bacteria was used, while the suitability of this approach was discussed. The expression of the 16S rRNA gene demonstrated ribosome formation in cells, thus the presence of live bacterial cultures was found in our samples. The expression of mecA gene, which is responsible for the emerging of resistance to β-lactam antibiotics, was demonstrated in two samples from eight. The expected result was to confirm the expression of this gene in commercially supplied MRSA, and further to confirm the presence

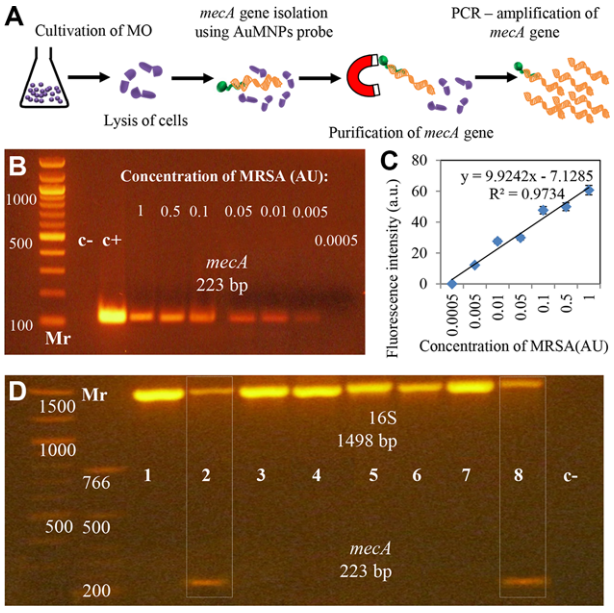

Figure 2. (A) General scheme of steps for cultivation of microorganisms, cell lysis, isolation of DNA by paramagnetic particles, and amplification of *mecA* gene for identification of MRSA inside of the 3D-printed chip using primers modified by gold nanoparticles (AuNPs). (B) Amplification of MRSA *mecA* gene by PCR with specific primers and its detection (λ_{600}). The numbers 1, 2, 3, 4, 5, 6, and 7 correspond to absorbance (λ_{600}) 0.0005, 0.005, 0.01, 0.05, 0.1, 0.5, 1 AU, respectively. C−, negative control (*S. aureus* without *mecA* gene); C+, positive control (MRSA with *mecA* gene). The reverse transcription in *mecA* gene for the confirmation of *mecA* gene expression in MRSA bacterial culture was made. (C) Dependence of MRSA concentration (0.0005, 0.005, 0.01, 0.05, 0.1, 0.5, 1 AU) on fluorescence intensity determined from gel electrophoresis. (D) The amplification of 16S and *mecA* genes by multiplex PCR with 16S and mecA primers in various PCR products of bacterial strains: (1) *S. aureus*, (2) MRSA, (3) *E. coli*, (4) *S. typhimurium*, (5) *L. rhamnosus* and three clinical specimens, where the presence of *S. aureus* was confirmed (sample numbers 6–8) and C− as a negative control. In all samples, the expression of 16S control gene was confirmed. In samples 2 and 8 the expression of *mecA* gene was also confirmed. The confirmation of the expression of 16S control gene and *mecA* gene was performed using multiplex PCR.

of such gene in the sample isolated from the hospital sample, which was identified as an *S. aureus*. Both assumptions were confirmed and the resistance to β-lactam antibiotics was found in MRSA obtained from the collection and also in clinical samples (Fig. 2D). In the other tested bacterial strains the *mecA* gene was not confirmed, therefore constituted nonmethicillin-resistant strains (Fig. 2D). Moussa and Shibl also used 16S rRNA and *mecA* genes for identification of MRSA [27]. Their study was expanded to include the presence of Panton-Valentine Leucocidin, which is a cytotoxin produced by community-associated MRSA bacterial strain [27], and are in good agreement with those found in our study.

3.3 Identification of *mecA* gene fragment to the AuNPs probe

The identification of *mecA* gene fragment is based on noncross-linking DNA hybridization method using the AuNPs probe and its ability to aggregate induced by an increasing salt concentration in the presence of complementary oligonucleotides of the same size [28]. The experimental scheme (Fig. 3A) shows that the *mecA* gene is bound to the AuNPs probe based on the bases complementarity. After the NaCl addition, the unbounded AuNPs probes aggregate. The colloidal solution of AuNPs exhibits a red color and their aggregation is driven by the London–van der Waals attractive force between the nanoparticles, and the color turns to purple red [28]. Based on these facts, we focused on the color change of AuNPs in the presence of MRSA *mecA* gene using the absorbance spectra measurement. Using the agarose gel electrophoresis, it was found that AuNPs probe contained *mecA* primers. Functionality of AuNPs probe bound to the *mecA* gene was proved by multiplex PCR visualized by electrophoresis on agarose gel (Fig. 3B). It is evident from the results shown in Fig. 3B that two bands of approximately same molecular weight of *mecA* gene were found in samples 2 and 8. These results confirmed the suitability of AuNPs probe for *mecA* gene detection because they are in perfect agreement with those shown in Fig. 2D.

Subsequently, we characterized the absorbance properties of AuNPs under various concentrations of NaCl (0–2 M). The AuNPs showed the immediate color change in low concentrations of NaCl. It follows from titration curve (Fig. 3C) that the rapid decrease of AuNPs absorbance in 530 nm in the presence of 0.125 M NaCl occurred and this decreasing trend progressed also with higher NaCl concentration.

Further, we used the described methods to analyze various PCR products of bacterial strains: (1) *S. aureus*, (2) MRSA, (3) *E. coli*, (4) *S. typhimurium*, (5) *L. rhamnosus* and three clinical specimens, where *S. aureus* presence (sample numbers 6–8) was confirmed. First, the isolation of DNA from the bacterial culture and subsequent PCR was carried out. Obtained PCR products were mixed with AuNPs probe functionalized with complementary sequence to *mecA* gene and after hybridization the 10 μL of 5 M NaCl was added into the mixture. We estimated that the color change in the case of AuNPs (0) turned transparent while the samples with noncomplementary DNA to AuNPs probe turned to purple red (samples 1 and 3–7). In the case of MRSA PCR products (2, 8), the mixture showed the stable pink color (Fig. 3D). The typical absorbance spectrum of AuNPs with absorbance maximum at 530 nm is shown in Fig. 3E. In the case of *S. aureus* PCR product, the addition of NaCl into the reaction mixture caused the rapid decrease of absorbance measured at 530 nm. On the other hand, the absorbance spectra of MRSA reaction mixture after NaCl addition shows almost 75% decrease of AuNPs absorbance maximum at 530 nm compared to AuNPs (100%). We analyzed the other bacterial strains in the same way. The absorbance decrease at 530 nm was observed in (3)

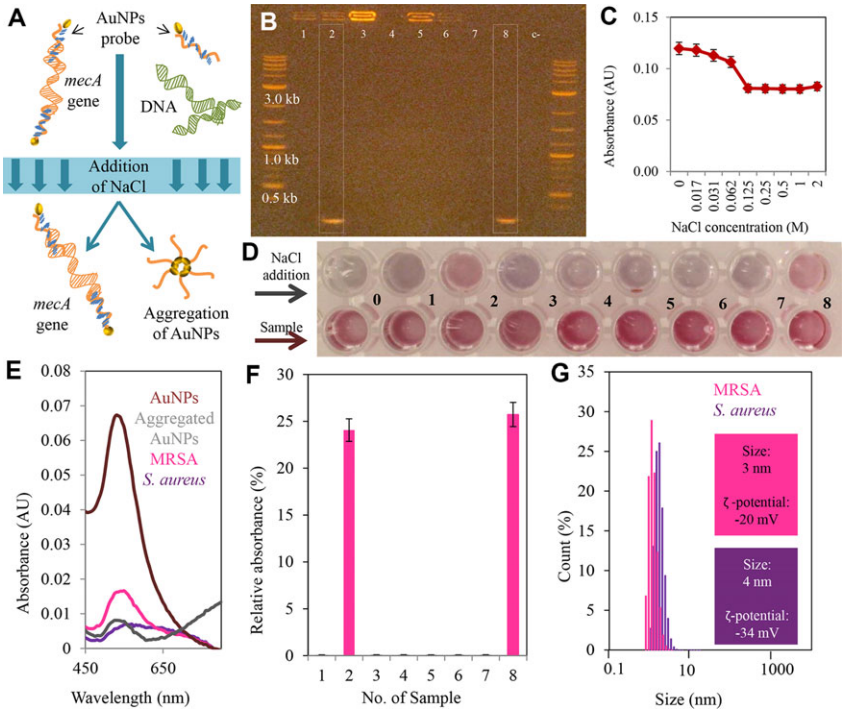

Figure 3. (A) Experimental scheme of *mecA* gene detection. (B) Amplification of *mecA* genes by PCR with AuNPs probe containing *mecA* primers in various PCR products of bacterial strains: (1) *S. aureus*, (2) MRSA, (3) *E. coli*, (4) *S. typhimurium*, (5) *L. rhamnosus* and three clinical specimens, where the presence of *S. aureus* was confirmed (sample numbers 6–8). In samples 2 and 8, the expression of *mecA* gene was confirmed. (C) Titration curve of AuNPs with addition of 0–2 M NaCl. The results are expressed as mean ± SD. (D) The color change of reaction mixtures before 2 M NaCl addition and after NaCl addition into sample: (0) AuNPs, (1) *S. aureus*, (2) MRSA, (3) *E. coli*, (4) *S. typhimurium*, (5) *L. rhamnosus* and three clinical specimens, where the presence of *S. aureus* was confirmed (sample numbers 6–8). (E) The absorbance spectra of reaction mixtures: AuNPs, AuNPs in 2M NaCl, MRSA, and *E. coli*. (F) Comparison of reaction mixtures relative absorbance: various PCR products of bacterial strains 1–8. The results are expressed as percentage of the AuNPs signal (100%). (G) Size distribution of AuNPs in mixture with MRSA (pink line) and *S. aureus* PCR products.

E. coli, (4) *S. typhimurium*, and (5) *L. rhamnosus*. For *S. aureus* (1; 6–7), nearly 90% decrease was observed (Fig. 3F). It follows from the results shown in Fig. 3G that there is a moderate increase in size of aggregated AuNPs in the presence of *mecA* gene to 3 and 4 nm in the case of negative control (*S. aureus* PCR product). Considerable change was visible in zeta potential results. Although the zeta potential of AuNPs in the presence of *mecA* gene was −20 mV, the zeta potential obtained from negative control increased to −34 mV. These results suggest that the AuNPs with sample mixture were weakly aggregated, and simultaneously stabilized the solution electrochemically.

3.4 Characterization of 3D-printed chip device and confirmation of detection inside the chip

Three-dimensional (3D) printed chips are among the new molecular techniques that rapidly monitor the presence of pathogen microorganisms [29, 30], which was demonstrated on detection of the bacterial strains in environment [31]. Their specificity, speed, and the ability to recognize a very low concentration of target molecules belong to the most important features of these chips [32].

In our study, individual steps preceding the detection were included to reaction chamber that was heated allowing the cultivation of microorganisms in Luria Bertani medium under constant conditions of 37°C and stirring. From these cultures, the DNA can be isolated using AuMNPs, and after this procedure the specific gene can be amplified using target primers whose presence can be spectrophotometrically detected by mixing with AuNPs probe and NaCl as an indicator

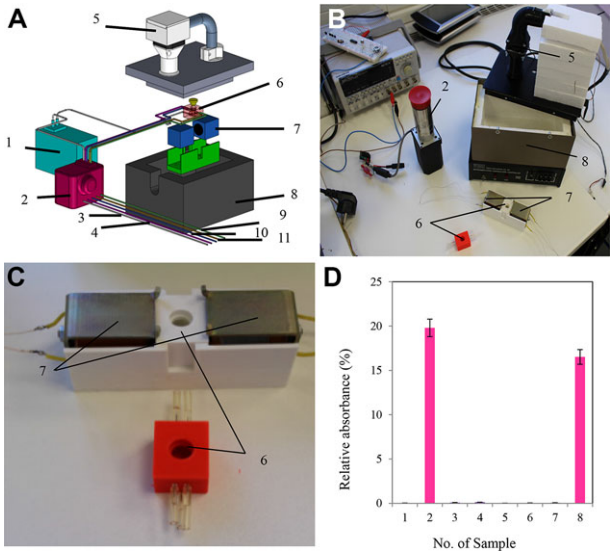

Figure 4. (A) Scheme of 3D-printed chip for detection and confirmation of MRSA presence using binding of MRSA to the gold nanoparticles with specific primers in the chip, (B) system for the identification of MRSA in the sample, and (C) reaction chamber of 3D-printed chip: 1—spectrophotometric detector, 2—pump with the valves, 3—outlet, 4—the first inlet hose, 5—thermoregulatory system, 6—cultivation chip, 7—electromagnet, 8—thermoisolating box, 9—the second inlet hose, 10—the third inlet hose, and 11—the fourth inlet hose. (D) Comparison of reaction mixtures relative absorbance obtained from 3D-printed chip: various PCR products of bacterial strains: (1) *S. aureus*, (2) MRSA, (3) *E. coli*, (4) *S. typhimurium*, (5) *L. rhamnosus* and three clinical specimens, where the presence of *S. aureus* was confirmed (sample numbers 6–8). The results are expressed as percentage of the AuNPs signal (100%).

of MRSA presence (Fig. 4A and B). The mixing and stirring during the bacterial cultivation was enabled using DNA-functionalized AuMNPs, which stirred up the liquids inside the chip. Electromagnets, visible from the picture (Fig. 4C), alternately changed its magnetic field, which resulted in movement of magnetic AuNPs. The magnetic field of electromagnets must be homogenous throughout the chip area, because magnetic particles are not concentrated only in the axis cores of electromagnets. The strength of the magnetic field must be sufficiently large and the time of the pulse, which controls the magnets, must be kept to a minimum. Magnetic particles must pulsate for the longest path. Using the control unit and electromagnets, it is possible to control magnetic particles movement in terms of speed and setting of different intervals of regular and irregular movements. For bacterial cultivation, the period of voltage on magnet connectors was set to 1 Hz. The whole cultivation process in the chip is maintained at a constant temperature of 37°C using a thermostatic box. At the end of the process, the control unit terminates the pulse of the electromagnets and maintains a constant direct current voltage on the terminals. Thus, the magnetic particles are at the right place and the lysis buffer is injected to the reaction chamber. The lysis inside the chip was carried out according to the protocol mentioned in Section 2.10.1. After the bacterial lysis, the purification of isolated DNA was done by rinsing the reaction chamber with water, while the AuMNPs probes functionalized by DNA were attached in magnetic field.

PCR as a second step was performed according to Section 2.10.3. The detection of PCR product inside the chip consisted, as in the case of absorbance detection using multifunctional reader, in the binding of the amplified PCR product (*mecA* gene) to AuNPs labeled by thiol oligonucleotide with specific affinity to gold and complementary sequence to *mecA* gene. The tested samples (1) *S. aureus*, (2) MRSA, (3) *E. coli*, (4) *S. typhimurium*, (5) *L. rhamnosus*, and three clinical specimens, which confirmed *S. aureus* presence (sample numbers 6–8), were subjected to analysis using our fabricated 3D-printed chip. The bacterial cultivation, PCR, and spectrophotometric detection were done by optimized protocols mentioned above. Spectrophotometric signal of tested samples at $\lambda = 530$ nm was expressed as percentage of the AuNPs signal (100%). It clearly follows from the results shown in Fig. 4D that the presence of MRSA was confirmed in samples 2 and 8, where 80% decrease of AuNPs absorbance compared to AuNPs was observed. In other samples, the absorbance decrease was almost 100% indicating the *mecA* gene absence. These results are in good agreement with our previous examination and proved our fabricated chip as a powerful tool for confirming the presence of MRSA.

4 Concluding remarks

Function of 3D-printed chip was tested on detection of *mecA* gene, which occurs in MRSA only. This colorimetric detection was based on specific binding of *mecA* gene to the AuNPs labeled with thiol oligonucleotides with complementary sequence. Due to this fact, we were able to prove the presence of two positive samples from eight. These samples probably contained the sequence of *mecA* gene, a gene encoding in MRSA strain, the resistance to β-lactam antibiotics. Therefore, we can assume that this platform may be used for rapid detection of a range of other microorganisms, in case, via labeling of AuNPs by thiol oligonucleotides with sequence complementary to specific genes in tested bacterial strains.

Financial support from the following project CEITEC CZ.1.05/1.1.00/02.0068 is highly acknowledged. The authors wish to express their thanks to Marie Konecna, Branislav Ruttkay-Nedecky for language correction, Roman Guran for MALDI analysis, Radek Chmela for perfect sample preparation, Lukas Melichar for X-ray fluorescence analysis, and Michal Zurek for scanning electrochemical microscope analysis.

The authors have declared no conflict of interest.

5 References

[1] Gould, I. M., *J. Hosp. Infect.* 2005, *61*, 277–282.

[2] Gould, I. M., *Int. J. Antimicrob. Agents* 2009, *34*, S8–S11.

[3] Agnoletti, F., Mazzolini, E., Bacchin, C., Bano, L., Berto, G., Rigoli, R., Muffato, G., Coato, P., Tonon, E., Drigo, I., *Vet. Microbiol.* 2014, *170*, 172–177.

[4] Higginbotham, K. L., Burris, K. P., Zivanovic, S., Davidson, P. M., Stewart, C. N., *Food Control* 2014, *40*, 274–277.

[5] Sadeghi, J., Mansouri, S., *Apmis* 2014, *122*, 405–411.

[6] Costa, A. M., Kay, I., Palladino, S., *Diagn. Microbiol. Infect. Dis.* 2005, *51*, 13–17.

[7] Francois, P., Pittet, D., Bento, M., Pepey, B., Vaudaux, P., Lew, D., Schrenzel, J., *J. Clin. Microbiol.* 2003, *41*, 254–260.

[8] House, D. L., Chon, C. H., Creech, C. B., Skaar, E. P., Li, D. Q., *J. Biotechnol.* 2010, *146*, 93–99.

[9] Focke, M., Stumpf, F., Faltin, B., Reith, P., Bamarni, D., Wadle, S., Muller, C., Reinecke, H., Schrenzel, J., Francois, P., Mark, D., Roth, G., Zengerle, R., von Stetten, F., *Lab Chip* 2010, *10*, 2519–2526.

[10] Shen, F., Du, W. B., Davydova, E. K., Karymov, M. A., Pandey, J., Ismagilov, R. F., *Anal. Chem.* 2010, *82*, 4606–4612.

[11] Koydemir, H. C., Kulah, H., Alp, A., Uner, A. H., Hascelik, G., Ozgen, C., *IEEE Sens. J.* 2014, *14*, 1844–1851.

[12] Wang, C. H., Lien, K. Y., Wu, J. J., Lee, G. B., *Lab Chip* 2011, *11*, 1521–1531.

[13] Bautista-Trujillo, G. U., Solorio-Rivera, J. L., Renteria-Solorzano, I., Carranza-German, S. I., Bustos-Martinez, J. A., Arteaga-Garibay, R. I., Baizabal-Aguirre, V. M., Cajero-Juarez, M., Bravo-Patino, A., Valdez-Alarcon, J. J., *J. Med. Microbiol.* 2013, *62*, 369–376.

[14] Predrag, S., Branislava, K., Miodrag, S., Biljana, M. S., Suzana, T., Natasa, M. T., Tatjana, B., *Braz. J. Microbiol.* 2012, *43*, 215–223.

[15] Bosch-Mestres, J., Martin-Fernandez, R. M., de Anta-Losada, M. T. J., *Enferm. Infecc. Microbiol. Clin.* 2003, *21*, 346–349.

[16] Lasch, P., Fleige, C., Stammler, M., Layer, F., Nubel, U., Witte, W., Werner, G., *J. Microbiol. Methods* 2014, *100*, 58–69.

[17] Chan, W. S., Tang, B. S. F., Boost, M. V., Chow, C., Leung, P. H. M., *Biosens. Bioelectron.* 2014, *53*, 105–111.

[18] Gultekin, A., Karanfil, G., Ozel, F., Kus, M., Say, R., Sonmezoglu, S., *J. Phys. Chem. Solids* 2014, *75*, 775–781.

[19] Kwon, S. J., Bard, A. J., *J. Am. Chem. Soc.* 2012, *134*, 7102–7108.

[20] Latus, A., Noel, J. M., Volanschi, E., Lagrost, C., Hapiot, P., *Langmuir* 2011, *27*, 11206–11211.

[21] Filez, M., Poelman, H., Ramachandran, R. K., Dendooven, J., Devloo-Casier, K., Fonda, E., Detavernier, C., Marin, G. B., *Catal. Today* 2014, *229*, 2–13.

[22] Hertz, H. M., Larsson, J. C., Lundstrom, U., Larsson, D. H., Vogt, C., *Opt. Lett.* 2014, *39*, 2790–2793.

[23] Tabrizi, A., Ayhan, F., Ayhan, H., *Hacettepe J. Biol. Chem.* 2009, *37*, 217–226.

[24] Mitra, M., Kandalam, M., Rangasamy, J., Shankar, B., Maheswari, U. K., Swaminathan, S., Krishnakumar, S., *Mol. Vis.* 2013, *19*, 1029–1038.

[25] Gardete, S., de Lencastre, H., Tomasz, A., *Microbiology (UK)* 2006, *152*, 2549–2558.

[26] Navarro-Noya, Y., Hernandez-Rodriguez, C., Zenteno, J. C., Buentello-Volante, B., Cancino-Diaz, M. E., Jan-Roblero, J., Cancino-Diaz, J. C., *Braz. J. Microbiol.* 2012, *43*, 283–287.

[27] Moussa, I. M., Shibl, A. M., *Saudi Med. J.* 2009, *30*, 611–617.

[28] Sato, K., Hosokawa, K., Maeda, M., *J. Am. Chem. Soc.* 2003, *125*, 8102–8103.

[29] Borchers, K., Weber, A., Hiller, E., Rupp, S., Brunner, H., Tovar, G. E. M., *Abstr. Pap. Am. Chem. Soc.* 2006, *232*, 460–460.

[30] Bernacka-Wojcik, I., Lopes, P., Vaz, A. C., Veigas, B., Wojcik, P. J., Simoes, P., Barata, D., Fortunato, E., Baptista, P. V., Aguas, H., Martins, R., *Biosens. Bioelectron.* 2013, *48*, 87–93.

[31] Jiang, X. R., Shao, N., Jing, W. W., Tao, S. C., Liu, S. X., Sui, G. D., *Talanta* 2014, *122*, 246–250.

[32] Krejcova, L., Nejdl, L., Rodrigo, M. A. M., Zurek, M., Matousek, M., Hynek, D., Zitka, O., Kopel, P., Adam, V., Kizek, R., *Biosens. Bioelectron.* 2014, *54*, 421–427.

